

VERIFICATION OF PROTON BEAM RANGE USING PHOTOPOLYMERIZED PMMA-BASED PLASTICS SCINTILLATOR*

GWANGSOO KIM, HONGJOO KIM

Kyungpook National University, South Korea

SUNGHWAN KIM

Cheongju University, South Korea

*Received 7 August 2024, accepted 12 November 2024,
published online 27 November 2024*

Due to the high linear energy transfer (LET) and a Bragg peak, proton radiation therapy enables targeted radiation treatment focused on cancer cells while reducing exposure to normal tissues. However, various studies are needed to measure proton energy accurately, as uncertainties can arise depending on the energy of the proton beam and the characteristics of human tissue. In this work, we developed an optical dosimeter to verify the range of the proton beam using a PMMA (poly-methyl methacrylate)-based tissue-equivalent plastic scintillator with a CMOS (complementary metal-oxide-semiconductor) camera. The Bragg peak position was confirmed through image processing after photographing the scintillation light generated during proton beam irradiation with the camera. Additionally, the correct Bragg peak was measured by correcting for the quenching effect of the scintillator. The proton beam's energy was adjusted using an aluminum degrader, and the experimental results were verified by comparing them with the Geant4 simulation. The relationship between the simulated and measured proton beam ranges was $R^2 = 0.99$, confirming the validity of KOMAC's (Korea Multi-purpose Accelerator Complex) 102 MeV proton beam for range verification.

DOI:10.5506/APhysPolBSupp.17.7-A6

1. Introduction

With the recent development of cancer treatment technology, radiation therapy has become widely used. In particular, proton radiation therapy has the advantage of providing intensive treatment to cancer cells while

* Presented at the 5th Jagiellonian Symposium on *Advances in Particle Physics and Medicine*, Cracow, Poland, June 29–July 7, 2024.

minimizing radiation damage to normal tissues due to the high linear energy transfer (LET) at the desired target and the Bragg peak [1]. Consequently, many studies and clinical applications are being considered [2, 3].

The Bragg peak is a phenomenon where a proton beam releases the most energy at a specific depth. By delivering the desired energy to cancer cells while reducing the energy delivered to surrounding normal tissues, side effects on normal tissues can be minimized, improving cancer treatment outcomes. For this reason, proton radiation therapy has excellent biological effects and enhances patients' quality of life [4]. Various studies are being conducted to improve the accuracy and effectiveness of proton radiation therapy. However, various uncertainties in proton beam therapy, such as the density of human tissues or the energy fluctuation of the proton beam, still need to be solved. Therefore, methods are required to minimize these uncertainties and increase treatment precision [5–7].

This study aims to verify an optical method for determining the proton beam range using a CMOS (complementary metal-oxide-semiconductor) camera and a PMMA (poly-methyl methacrylate)-based tissue-equivalent plastic scintillator bar. PMMA is a polymer of methyl methacrylate with the chemical formula ($C_5H_8O_2$) and a density of 1.17–1.20 g/cm³ [8]. PMMA is capable of transmitting up to 92% of visible light through a thickness of 3 mm [9]. In conventional radiotherapy, the properties of the beam were mainly evaluated using ionizers, films, and physical detectors. However, these methods often have the disadvantage of high uncertainty or requiring complicated equipment. Due to the various advantages of scintillators, volumetric scintillation dosimetry has been proposed in several studies [10–12].

Measuring beam range with a scintillator has potential medical applications. Methods that could utilize scintillator beam monitoring include the Jagiellonian PET (J-PET) and INSIDE (Innovative Solution for Dosimetry in Hadron therapy) systems. The J-PET system employs plastic scintillators with fast timing signals, minimizing saturation issues and supporting precise in-beam monitoring. The INSIDE system employs Lutetium Fine Silicate (LFS) crystals and Silicon Photomultipliers (SiPMs) to monitor proton and carbon ion beam effectively ranges with millimeter accuracy during treatments [13]. Additionally, FLASH therapy may introduce measurement distortions when using an ionization chamber due to ion recombination caused by the high dose rate. Scintillator detectors, especially plastic ones, have advantages with their fast response, high radiation tolerance, and suitability for real-time monitoring, making them a promising option for precise dose tracking during FLASH therapy [14].

The thin, long cylindrical scintillator used in this study reduces internal scattering and offers a more compact design. The Bragg peak of the PMMA-based plastic scintillator was confirmed to be proportional within the proton

energy range reduced by the 100 MeV protons and the 2 mm aluminum degrader used in the experiment. The Bragg peak can be visually identified using the scintillator in proton beam radiotherapy. This can be captured as a digital image using a CMOS camera with excellent position resolution and fast response time. By combining these systems, we propose a method to monitor and evaluate the range of the proton beam in real time.

2. Material and methods

In this study, a photopolymerized PMMA-based plastic scintillator absorbed high-energy proton beam energy and subsequently emitted scintillation light. This emitted light was captured as an image through a CMOS camera. The experiment was carried out using the following procedure.

To produce PMMA-based tissue-equivalent plastic scintillators by photopolymerization, 0.20 wt% PPO (2,5-Diphenyloxazole, CAS Number: 92-71-7, Sigma-Aldrich Co.) was added to the liquid MMA monomer (methyl methacrylate, CAS Number: 80-62-6, Sigma-Aldrich Co.) as a primary solute. Additionally, 0.01 wt% POPOP (1,4-Bis(5-phenyl-2-oxazole)-benzene, CAS Number: 1806-34-4, Sigma-Aldrich Co.) was added as a wavelength shifter, and 0.20 wt% Irgacure 819 (Phenyl-bis(2,4,6-trimethylbenzoyl) phosphine oxide, BASF Co.) was added as a photoinitiator. The mixed solution was transferred into a cylindrical vial comprising neutral borosilicate glass material. When the emitted scintillation occurs in a 4π direction, a square cross section is asymmetric, while a circular cross section is symmetric. Therefore, a circular shape, symmetric with respect to the radiation beam center, is more advantageous for measurements. Figure 1 (a) shows the tissue-equivalent PMMA plastic scintillators photopolymerized with UV

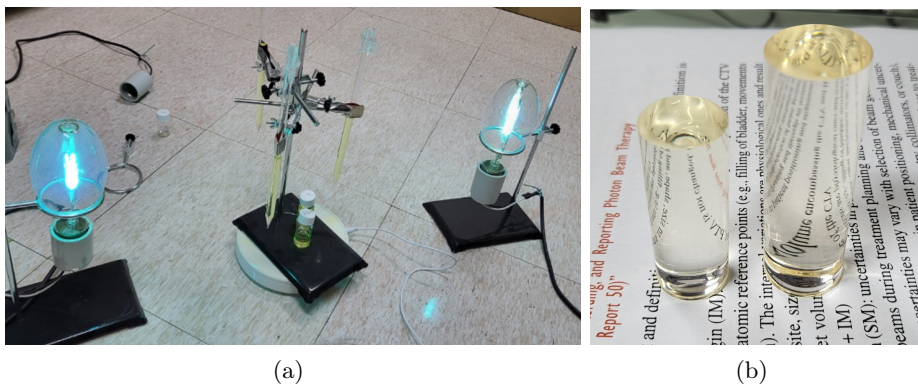


Fig. 1. (a) Setup for photopolymerization of plastic scintillator experiments with mercury lamps on the side of the vial. (b) Fabricated PMMA-based plastic scintillator.

mercury lamps. A 200 W mercury lamp was positioned approximately 50 cm from the vials and left for a full day to ensure sufficient polymerization. The surface of the scintillator was initially cut using a cutting tool, followed by polishing with progressively finer grades of sandpaper. Final polishing was conducted with aluminum oxide and a polishing cloth. Figure 1 (b) is a photograph of two photopolymerized PMMA plastic scintillators.

The emission spectrum for X-rays of the polymerized PMMA plastic scintillator was measured with a fiber-optic spectrophotometer (Avaspec-ULS2048LTEC, Avantes Co.) excited by X-rays (electron energy = 3 GeV, beam current = 251.43 mA) in PAL-II (Pohang Accelerator Laboratory). The scintillation properties of the PMMA scintillators were evaluated using 100 MeV proton beams (TR-102) at KOMAC (Korea Multi-purpose Accelerator Complex).

Figure 2 shows the layout and photograph of the PMMA plastic scintillator and CMOS camera for the KOMAC 100 MeV high-energy proton beam to evaluate the scintillation properties. The plastic scintillators, with a diameter of 2 cm and a length of 20 cm, sufficient to deposit 100 MeV proton energy, were placed parallel to the incident direction of the proton beam in the dark box. The scintillation light generated from the plastic scintillator by proton beams was photographed as a digital image with a CMOS (ASI120MM, ZWO Co.) camera combined with a commercial lens (focal length = 125 mm and F2.0) in the vertical direction and dose evaluation was performed through analysis of the images using ImageJ ver. 1.65a (National Institutes of Health, USA). The energy of the proton beam was adjusted using 2.0 cm Al degraders. To minimize the effect of scattering, a collimator with a 10 mm diameter and 50 mm thickness was placed in front of the plastic scintillator. The distance between the beam window and the scintillator was set to 2 m, and the Geant4 Monte Carlo simulation and the optical dosimetry results were compared and evaluated under these conditions.

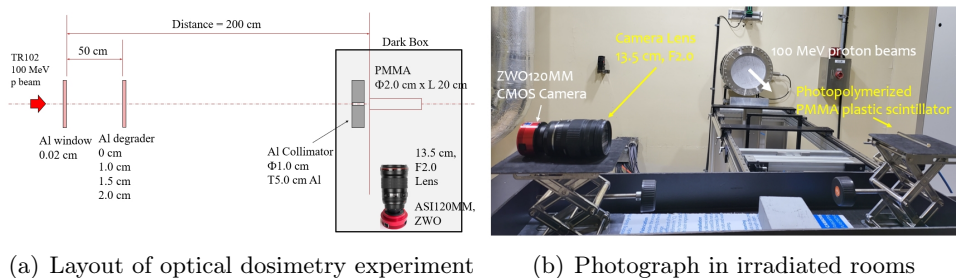


Fig. 2. (a) The plastic scintillator detector system. (b) The plastic scintillator and the PMT inside of the brass box.

A background noise removal filter was applied to the images, pixel size correction was performed to correct the actual size, and a sharpening mask filter was used to increase the sharpness of the images. For the final processed images, the beam profiles were obtained from the pixel values according to the incident direction of the proton beams and compared and verified with the **Geant4** simulation results. In the scintillator, a quenching effect occurs, where the ratio of the amount of scintillation light to the energy of the incident radiation decreases depending on the type or energy of the detected radiation, leading to a reduction in pixel value in the resulting images [15]. By applying Birks' equation to correct the quenching effect, the proton beam's value is corrected, and finally, the range of the proton beam is determined.

3. Results and discussion

3.1. Scintillation properties

Figure 3 shows an emission spectrum generated when irradiated radiation is applied to the manufactured PMMA-based plastic scintillator. The emission spectrum ranges from 360 to 500 nm, with maximum peaks at 411 nm. This is comparable to the emission peaks observed in polystyrene and polyvinyl toluene scintillators doped with POPOP, which exhibit peak wavelengths of 422 nm and 425 nm, respectively [16, 17]. Figure 4 shows the linearity of the PMMA-based plastic scintillator according to the proton beam currents. It demonstrates excellent linearity with an R^2 value of 0.98 within the dose rate range.

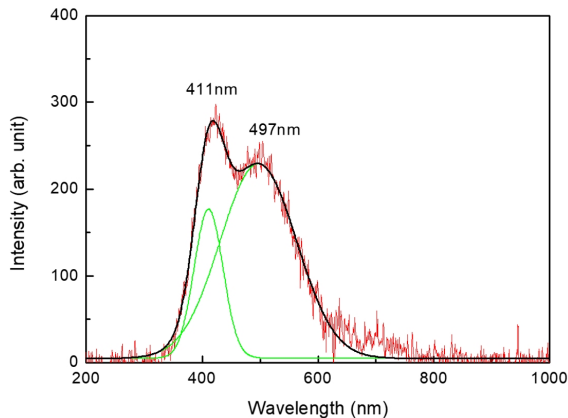


Fig. 3. Emission spectrum of the photo-polymerized PMMA plastic scintillator excited by X-ray in PAL-II. The green line represents the deconvolution of the peaks.

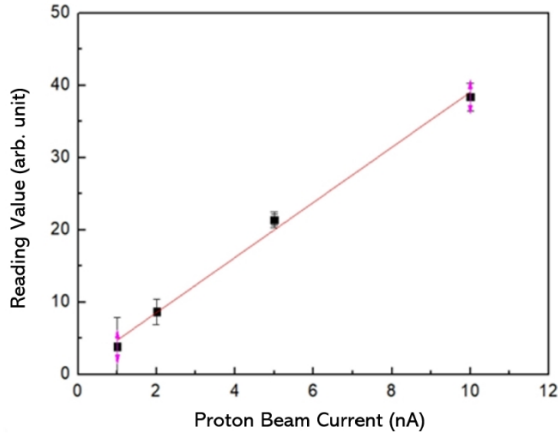


Fig. 4. Dose rate dependency of the PMMA plastic scintillator to the proton beam currents.

3.2. Optical dosimetry

Figure 5 shows images taken with a CMOS camera of the scintillation lights generated when irradiating a PMMA scintillator with Al degraders of varying thicknesses (none, 10 mm, 15 mm, and 20 mm) for a 102 MeV proton beam to change the proton beam energy. The images were taken using optical zoom from 1.5 m away to minimize optical distortion and vignetting by the lens. In Fig. 5, the Bragg peak can be observed due to the amount of scintillation light generated within the 20 cm long PMMA plastic scintillator. Additionally, as the thickness of the aluminum degrader increases, the proton beam's energy decreases, and consequently, the Bragg peak position shifts. Significant noise is generated in the image due to scattering

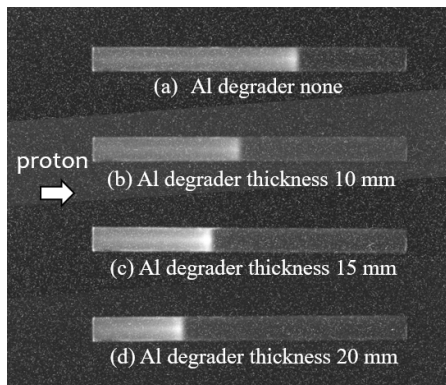


Fig. 5. Scintillation light distribution images of the proton beam according to the Al degraders taken with the ZWO CMOS camera.

rays produced by high-energy protons in the proton irradiation room. Flat image correction and noise removal filters were applied to mitigate this, and sharpening filtering was performed to enhance the image resolution.

Figure 6 (a) shows images of the pixel value profiles normalized to the peak using ImageJ (ver. 1.52a, NIH USA) for the plastic scintillator part of the processed image. Figure 6 (b) displays the normalized Bragg curves according to the thickness of the Al degrader as determined by the Geant4 simulation. The profile of the pixel values of the processed images measured by the scintillator matches well with the position of the Bragg peak according to the proton energy calculated from the Geant4 simulation. However, a quenching phenomenon occurs in scintillators, resulting in the loss of linearity between the amount of scintillation and the energy transfer. Since charged particle radiation loses energy while interacting with the material, the LET increases as the speed of the charged particle gradually slows down, necessitating quenching corrections [18].

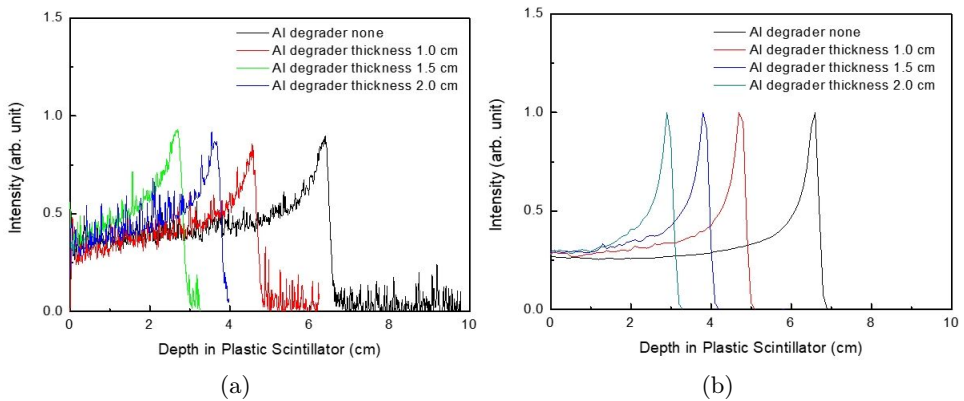


Fig. 6. (a) Normalized Bragg curves of the proton beam obtained by the amount of scintillation depending on the thickness of the Al degrader. (b) Normalized Bragg curves of the proton beam obtained by Geant4 simulation, depending on the thickness of the Al degrader.

3.3. Quenching effect correction

The quenching effect stands out when the LET is high. To measure the Bragg curve accurately, the quenching effect must be corrected in the profile of the pixel value of Fig. 6 (a). According to Birks' law, the following equation can explain the quenching effect [19]:

$$\frac{dL}{dx} = S \frac{\frac{dE}{dx}}{1 + kB \frac{dE}{dx}}.$$

Here, kB is called Birk's coefficient and is determined by the material's inherent properties, S is the scintillation efficiency, L is the light yield, and dE/dx is the energy loss of the particle per path length. According to this equation, the higher the dE/dx , the lower the conversion rate to light compared to when the quenching effect is not applied. This study did not consider the S value since the quenching effect was corrected at a relative ratio.

In the **Geant4** simulation, the proton beam determined the absorption energy at each PMMA depth. A value of 0.1 mm/MeV was used with reference to the kB value of a typical organic scintillator [20]. The quenching effect correction ratio was determined by applying this value to dE/dx according to the depth obtained by the simulation. Since the pixel value obtained from the image captured with CMOS is the value of the light yield reduced due to quenching, the pixel value was corrected by applying the quenching effect correction at the corresponding depth. The Bragg curve measured in Fig. 7 results from the correction of the quenching effect on the 102 MeV proton beam without the Al degrader in Fig. 6, and it agrees very well with the simulation results.

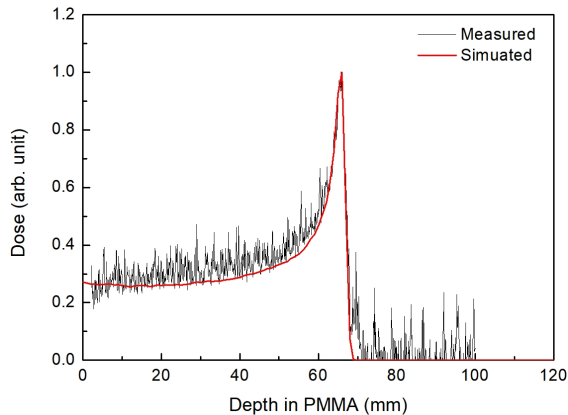


Fig. 7. Comparison of the Bragg curve of 102 MeV proton beam between corrected for quenching effect and obtained by the **Geant4** Monte Carlo simulation.

Figure 8 shows the correlation between the position of the Bragg peak obtained from the image taken using a CMOS camera and calculated with a **Geant4** simulation after adjusting the energy of the proton beam using the 0 cm, 1 cm, 1.5 cm, and 2 cm Al degraders for the 102 MeV proton beam. The calculation and measurement results within the experimental range show a very high correlation with $R^2 = 0.99$, and it was confirmed that the optical dosimetry method of the luminescent image using the CMOS camera proposed in this study can be usefully used to identify the Bragg peak position. Additionally, the PMMA material used as a scintillator is thought

to play an essential role in improving the accuracy of proton radiation treatment because the absorption dose can be directly measured with a substance like human tissue.

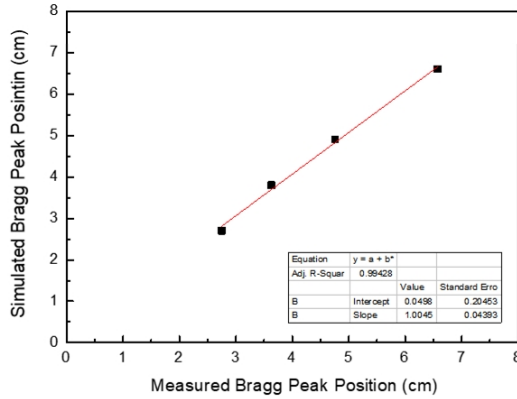


Fig. 8. Comparison of the Bragg peak position of proton beams according to the Al degrader thickness between measured from images by a CMOS camera and obtained by the Geant4 Monte Carlo simulation.

This study made more accurate analysis possible by improving the image quality through pixel size correction, noise removal, and sharpening mask treatment in the photometric data using the scintillator. In particular, the process of calibrating the quenching effect has contributed to improving the accuracy of the measurements by accurately understanding and reflecting the properties of the scintillators.

4. Conclusions

In this study, we present a new method to verify the range of the proton beam using a tissue-equivalent PMMA plastic scintillator bar fabricated by photopolymerization and a CMOS camera. It was verified through the Geant4 simulation that proton energy can be measured using the Bragg peak range. This non-invasive method can play an essential role in improving the accuracy of radiation therapy by allowing the Bragg peak position to be identified in real time. Future research may enable more precise measurements by enhancing the performance of various scintillator materials and CMOS cameras. These studies can contribute to increasing the efficiency and accuracy of radiation therapy and improving patients' quality of life.

Additionally, 3D printers using PMMA as a base for medical purposes have recently been in the spotlight. PMMA-based 3D printing typically involves extrusion or stereolithography. In extrusion, PMMA filament is heated and extruded layer by layer to form the desired object. In stere-

olithography, a resin containing PMMA is selectively cured using UV light. It is expected that the utility of PMMA for medical purposes will increase in the future [21, 22].

The authors acknowledge the financial support of the National Research Foundation of Korea (NRF), funded by the Ministry of Science and Technology, Korea, under project NRF No. 2018R1A6A1A06024970. This work was also supported by the MC-50 Cyclotron Laboratory (KIRAMS), and the authors express their sincere thanks to the staff of KOMAC (Korea Multi-purpose Accelerator Complex) for their support during the experiment.

REFERENCES

- [1] H. Paganetti, P. Luijk, *Semin. Radiat. Oncol.* **23**, 77 (2013).
- [2] K.J. Gallagher *et al.*, *Int. J. Part. Ther.* **7**, 1 (2021).
- [3] V. Verma *et al.*, *Radiother. Oncol.* **125**, 21 (2017).
- [4] O. Jäkel, *AIP Conf. Proc.* **958**, 70 (2007).
- [5] H. Paganetti, *Phys. Med. Biol.* **57**, R99 (2012).
- [6] G. Lucconi *et al.*, *Radiat. Med. Protect.* **2**, 95 (2021).
- [7] L. Archambault *et al.*, *Int. J. Radiat. Oncol. Biol. Phys.* **78**, 280 (2010).
- [8] M. Mozafari, N.P.S. Chauhan, «Handbook of Polymers in Medicine», Elsevier, 2003.
- [9] L.W. McKeen, «The Effect of UV Light and Weather on Plastics and Elastomers», Elsevier, 2019.
- [10] A.S. Kirov *et al.*, *Phys. Med. Biol.* **50**, 3063 (2005).
- [11] F. Pönisch *et al.*, *Med. Phys.* **36**, 1478 (2009).
- [12] Y. Fukushima, M. Hamada, T. Nishio, K. Maruyama, *Phys. Med. Biol.* **51**, 5927 (2006).
- [13] K. Parodi, T. Yamaya, P. Moskal, *Zeit. Med. Phys.* **33**, 22 (2023).
- [14] D.S. Levin *et al.*, *Med. Phys.* **51**, 2905 (2024).
- [15] M.R. Raju, «Heavy Particle Radiotherapy», New York: Academic Press, 1980.
- [16] Ł. Kapłon, G. Moskal, *Bio-Algorithms Med-Systems* **17**, 191 (2021).
- [17] L. Alex, R. Paulraj, Sonu, M. Tyagi, *J. Mater. Sci.: Mater. Electron.* **34**, 127 (2023).
- [18] T.A. Laplace *et al.*, *Mater. Adv.* **3**, 5871 (2022).
- [19] L.F. Nascimento *et al.*, *Sens. Actuators A: Phys.* **345**, 113781 (2022).
- [20] V.I. Tretyak, *Astropart. Phys.* **33**, 40 (2010).
- [21] M. Yousfia, A. Belhadja, K. Lamnawar, A. Maaouzoua, «3D printing of PLA and PMMA multilayered model polymers: an innovative approach for a better-controlled pellet multi-extrusion process», presented at the 24th International Conference on Material Forming ESAFORM2021, 10.25518/esaform21.1024.
- [22] E. Marin *et al.*, *Mater. Today Commun.* **32**, 103943 (2022).